

**COALESCENCE OF TWO CURRENT LOOPS WITH A KINK
INSTABILITY SIMULATED BY A 3-D EM PARTICLE CODE**K. Nishikawa ¹, J. Sakai ², J. Zhao ², T. Neubert ³, and O. Buneman ⁴¹ *Department of Physics and Astronomy, The University of Iowa,
Iowa City, Iowa 52242, U.S.A.*² *Laboratory for Plasma Astrophysics and Fusion Sciences,
Department of Electronics and Information, Faculty of Engineering,
Toyama University, Toyama 930, Japan*³ *Space Physics Research Laboratory, The University of Michigan,
Ann Arbor, Michigan 48109, U.S.A.*⁴ *STAR Laboratory, Stanford University,
Stanford, California 94305, U.S.A. (deceased January 24, 1993)***Abstract**

We have studied the dynamics of a coalescence of current loops using a 3-D electromagnetic (EM) particle simulation code. Our focus is the investigation of kinetic processes such as energy transfer, heating of particles, and electromagnetic emissions associated with a current loop coalescence which cannot be studied by MHD simulations. First, the two loops undergo a pinching oscillation due to a pressure imbalance between the inside and outside of the current loop. During the pinching oscillation, a kinetic kink instability is excited and electrons in the loops are heated perpendicularly to an ambient magnetic field. Next, the two current loops collide and coalesce, while at the same time a helical structure grows further. Subsequently, the perturbed current, which is due to these helically bunched electrons, can drive a whistler instability. It should be noted in this case that the whistler wave is excited by the kinetic kink instability and not a beam instability. After two helical loop coalescence tilting motions can be observed in the direction of left-hand rotation, and the helical structure will relax resulting in strong plasma heating mostly in the direction perpendicular to the ambient magnetic field.

1. Introduction

Recent soft X-ray images observed by the 'Yohkoh' satellite showed many coronal loop structures in the active regions of the lower corona, which changes dynamically through the loop-loop interaction (Shimizu et al. 1992). Some solar flares showed evidence that during the impulsive phase, two current loops collided with each other as also observed by 'Yohkoh' (Inda-Koide et al. 1993; Takahashi et al. 1993). Gold & Hoyle (1960) first proposed the idea to explain the solar flare by the loop coalescence process. Tajima, Brunel, & Sakai (1982) showed that strong particle acceleration occurs during the two loop coalescence using 2-D particle code simulations, and the results were applied to solar flares (Tajima et al. 1987;

Sakai & Ohsawa 1987; Sakai 1990). Recently current loop coalescence processes have been extended to many other aspects (Sakai and de Jager 1991; Chargeishvili et al. 1993; Zhao et al. 1993, 1994a) to explain the recent solar flares observed by 'Yohkoh'. Until now most work on current loop coalescence was done mainly by 2-D MHD codes (Pritchett & Wu 1979; Biskamp & Welter 1980; Brunel et al. 1982; Bhattacharjee et al. 1983; Tajima & Sakai 1989a) and 2-D particle codes (Dickman et al. 1969; Leboeuf et al. 1982; Tajima et al. 1987; Tajima & Sakai 1989a,b; Pritchett 1992) as well as 3-D MHD codes (Koide & Sakai 1993).

Recently a new 3-D electromagnetic particle code (Buneman, 1994) has been developed and applied to several problems (Neubert et al. 1992; Buneman et al. 1992; Zhao et al. 1994b; Nishikawa et al. 1994a). Here we use the same code with some modifications such as the initial conditions to investigate the dynamical development of current loop coalescence.

2. Simulation model and Loop coalescence

The system size used for the simulations is $L_x = L_y = 85\Delta$, $L_z = 160\Delta$, where L_x , L_y , and L_z are the lengths of the system in three dimensions and $\Delta (= 1)$ is the grid size. We use a million electron-ion pairs. Periodic boundary conditions are used along the ambient magnetic field (z -direction), while radiating boundary conditions (Lindman 1975) are used in the x - and y -directions.

The electrons carrying two loop current are initially in two columns oriented along the z -direction with radius $a = 4\Delta$, and the two centers are located at $x_{c1} = 32$, $y_{c1} = 43$, and $x_{c2} = 52$, $y_{c2} = 43$. The plasma density within the current column is the same as outside. The numbers of current electrons within the columns are 7780 and 7789, respectively. The electron drift velocity of both currents is the same and $V_d = 7.0v_{et}$ ($0.66c$), where v_{et} is the electron thermal velocity and $c = 0.5$. The electron temperature associated with the currents is $T = 0.09T_b$, where T_b is the temperature of the background electrons. We chose the following: $m_i/m_e = 64$, $T_e/T_i = 1$, $\Omega_e/\omega_{pe} = 0.4$, $c/v_{et} = 10.67$, $\omega_{pe}\Delta t = 0.10$, $\beta = 0.111$, $\lambda_{De} = 0.469\Delta$, $\rho_e = 1.17\Delta$, $\rho_i = 9.38\Delta$, and $c/\omega_{pe} = 5.00\Delta$.

The ambient magnetic field is $B_{z0} = 0.1$. Quiet start conditions are achieved by including an initial poloidal magnetic field consistent with the current density J_z carried by the electrons in the two columns at $\omega_{pe}t = 0$ (Nishikawa et al. 1994a). The maximum ratio between the poloidal and ambient magnetic fields at the edge of the column is $B_\theta/B_{z0} = 0.8$.

In this section we will show the simulation results of the two current loop coalescence process. The detailed results should be referred to (Nishikawa et al. 1994b). We can classify the dynamical behavior of the two current loop coalescence into three phases: (1) pinching oscillation of each current loop, (2) excitation of a kinetic kink instability with helical perturbations, and (3) coalescence and relaxation associated with perpendicular heating of the particles. As seen in Figure 1, each current loop can undergo a pinching oscillation due to the pressure imbalance between the inside and outside of the loops until $\omega_{pe}t = 20$. In the second phase following the pinching oscillation, a kinetic kink instability is dominantly excited. The helical perturbations with left-hand polarization can be driven by this instability. The mode number calculated by $krB_z(r)/B_\theta(r) = 1$, $k \equiv 2\pi/L$ ($r = a$, $n = 8$) shows good agreement with simulation results. In this simulation the Alfvén velocity is $V_A/c = (m_e/m_i)^{1/2}\Omega_e/\omega_{pe} = 0.05$. We can get the Alfvén transit time $\tau_A = a/V_A = 16\omega_{pe}^{-1}$ using $a = 4\Delta$. Therefore, the growth time of the kinetic kink instability observed in the simulation is consistent with the Alfvén transit time.

Figure 1 shows the time history of the three components of the electric field as well as the magnetic field energies for the two loop case. For the single loop case, a pinching and expansion takes place repeatedly (Sakai et al. 1994). Then helical perturbations grow and due to the helically bunched beam electrons a beam-like instability is excited. Before the two loops approach each other at about $\omega_{pe}t = 18$, two current loops repeat pinching and expansion (as the single loop), and therefore, the electric field energies E_x^2 and E_y^2 oscillate as seen in Figure

1.

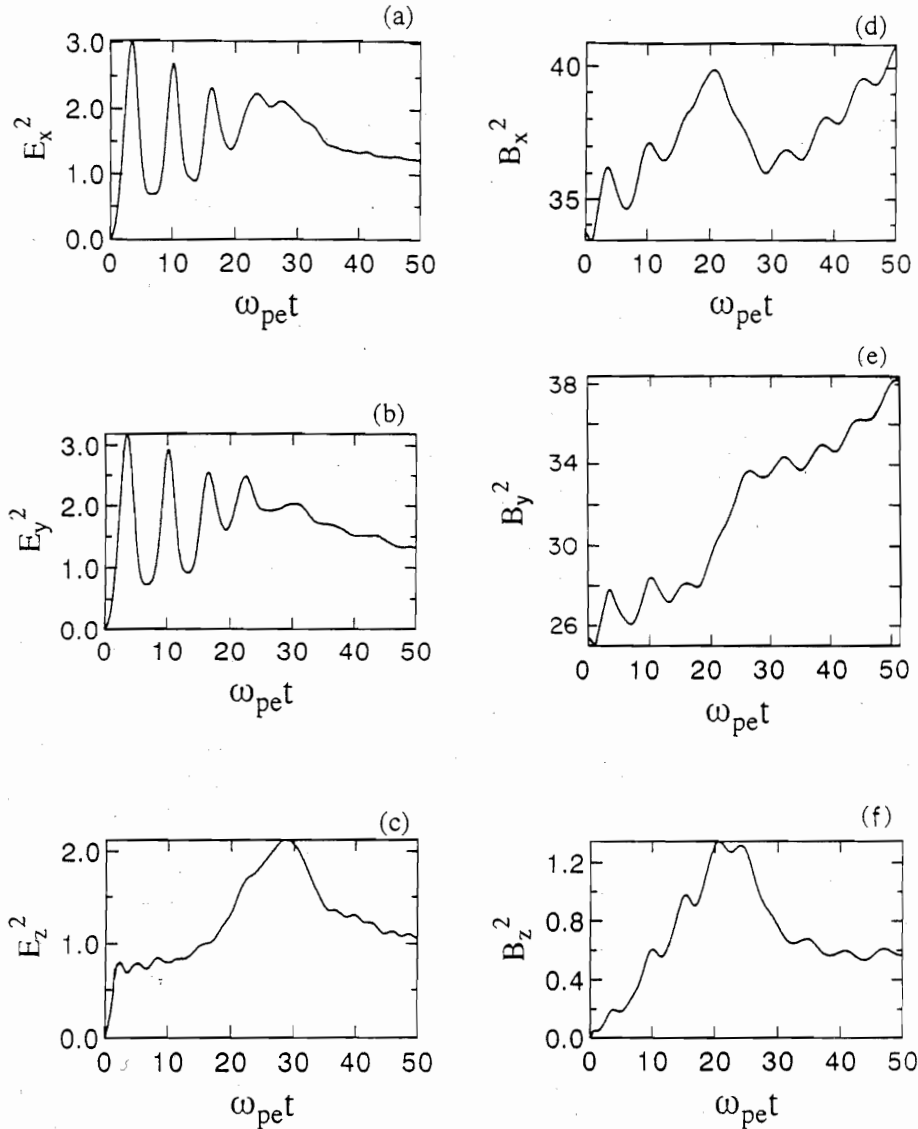


Fig. 1. Time history of the perturbed field energy in the simulation system, (a) E_x^2 , (b) E_y^2 , (c) E_z^2 , (d) B_x^2 , (e) B_y^2 , (f) B_z^2 .

The oscillations of E_x^2 and E_y^2 are due to the pinching. The pinching motion is strong and followed by the kinetic kink instability. For the B_y^2 case, the initial value is smaller than the B_x^2 because the B_y is cancelled out between the two current loops. Furthermore, due to the coalescence the B_y^2 increases rapidly after $\omega_{pe}t = 20$, and continues to increase monotonically different from B_x^2 . The B_z^2 energy grows more quickly and reaches a much higher level due to the current loop coalescence.

3. Summary and discussion

We have presented simulation results of the two current loop coalescence by using a 3-D electromagnetic particle code. The dynamical behavior of the two loop collision can

be classified into three phases: (1) pinching oscillation of each current loop, (2) excitation of a kinetic kink instability with helical perturbations, and (3) plasma heating due to current loop coalescence and high-frequency electromagnetic wave emission. It was shown that the dc electric current can be dissipated through a pinching oscillation and the electrons are heated mostly in the direction perpendicular to the magnetic field. The dc electric current can generate a kinetic kink instability with strong density perturbations. The temperature anisotropy produced by the pinching oscillation can also induce high-frequency electromagnetic waves strongly in the direction of the electron drift velocity (Zhao et al. 1994a). After a two loop coalescence both electrons and ions can be further heated, resulting in the initial current dissipation. The electrons originally inside the current column can be heated about 50 times compared with the initial temperature in the direction perpendicular to the magnetic field.

References

1. Bhattacharjee, A., Brunel, F., & Tajima, T. 1983, *Phys. Fluids*, **26**, 3332.
2. Biskamp, D. & Welter, H. 1980, *Phys. Rev. Lett.*, **44**, 1069.
3. Brunel, F., Tajima, T. & Dawson, J.M. 1982, *Phys. Rev. Lett.*, **49**, 323.
4. Buneman, O. 1994, in *Computer Space Plasma Physics, Simulation Techniques and Softwares*, edited by H. Matsumoto and Y. Omura (Terra Scientific, Tokyo) p. 1, in press.
5. Buneman, O., Neubert, T., & Nishikawa, K.-I. 1992, *IEEE Trans. Plasma Sci.*, **PS-20**, 810.
6. Chargeishvili, B., Zhao, J., & Sakai, J.I. 1993, *Solar Phys.*, **145**, 297.
7. Dickman, D.O., Morse, R. L., & Nielson, C. W. 1969, *Phys. Fluids*, **12**, 1708.
8. Gold, T. & Hoyle, F. 1960, *M.N.R.A.S.*, **120**, 89.
9. Inda-Koide, M., Sakai, J.I., Koide, S., Zhao, J., Shimizu, T., & Kosugi, T. 1993, submitted to *Pub. Astro. Soc. Jpn.*
10. Koide, S., & Sakai, J.I. 1993, *Solar Phys.*, in press.
11. Leboeuf, J. N., Tajima, T., & Dawson, J. M. 1982, *Phys. Fluids*, **25**, 784.
12. Lindman, E. L. 1975, *J. Comput. Phys.*, **18**, 66.
13. Neubert, T., Miller, R.H., Buneman, O., & Nishikawa, K.-I. 1992, *Geophys. Res.*, **97**, 12,057.
14. Nishikawa, K.-I., Buneman, O., & Neubert, T. 1994a, *Geophys. Res. Lett.*, in press.
15. Nishikawa, K.-I. Sakai, J.I. Zhao, J. Neubert, T. & Buneman, O. 1994b, *Ap. J.*, submitted.
16. Pritchett, P.L. 1992, *Phys. Fluids*, **B4(10)**, 3371.
17. Pritchett, P.L. & Wu, C.C. 1979, *Phys. Fluids*, **22**, 2140.
18. Sakai, J.I. 1990, *Ap. J.*, **365**, 354.
19. Sakai, J.I. & de Jager, C. 1991, *Solar Phys.*, **134**, 329.
20. Sakai, J.I., Zhao, J., & Nishikawa, K.-I. 1994, *Solar Phys.*, submitted.
21. Sakai, J.I. & Ohsawa, Y. 1987, *Space Science Rev.*, **46**, 113.
22. Shimizu, T., Tsuneta, S., Acton, L.W., Lemen, J.R., & Uchida, Y. 1992, *Pub. Astro. Soc. Jpn.*, **44**, L147.
23. Tajima, T., Brunel, F., & Sakai, J.I. 1982, *Ap. J.*, **258**, L45.
24. Tajima, T., Sakai, J.I., Nakajima, H., Kosugi, T., Brunel, F., & Kundu, M.R. 1987, *Ap. J.*, **321**, 1031.
25. Tajima, T. & Sakai, J.I. 1989a, *Soviet J. Plasma Phys.*, **15**, 519.
26. Tajima, T. & Sakai, J.I. 1989b, *Soviet J. Plasma Phys.*, **15**, 606.
27. Takahashi, M., Sakai, J.I., Nitta, N., Enome, S., Tsuneta, S., & Watanabe, T., 1993, *Pub. Astro. Soc. Jpn.*, submitted.
28. Zhao, J., Chargeishvili, B., & Sakai, J.I. 1993, *Solar Phys.*, **147**, 131.
29. Zhao, J., Sakai, J.I., & Nishikawa, K.-I. 1994a, *Solar Phys.*, to be submitted.
30. Zhao, J., Nishikawa, K.-I., Sakai, J.I., & Neubert, T., 1994b, *Phys. Plasmas*, **1**, 103.